Volume 48(1-4):25-33, 2004
Acta Biologica Szegediensis
http://www.sci.u-szeged.hu/ABS

ARTICLE

Competitive binding of quinone and antibiotic stigmatellin to reaction centers of photosynthetic bacteria

László Gerencsér[1], László Rinyu[1], László Kálmán[1], Eiji Takahashi[2], Colin A. Wraight[2], Péter Maróti[1]*

[1]Department of Biophysics, University of Szeged, Szeged, Hungary, [2]Department of Biochemistry and Center for Biophysics and Computational Biology, University of Illinois at Urbana-Champaign, Urbana, IL, USA.

ABSTRACT Stigmatellin bound to the Q_B site of the reaction center of photosynthetic bacteria is one of the most potent inhibitors of interquinone electron transfer. In addition to its inhibitory effect, it can be used to model protonated semiquinone and to probe the electrostatic environment. These properties were studied by two independent methods in isolated reaction centers and in chromatophores from cytochrome c-less mutant of *Rhodobacter sphaeroides*. The binding of the stigmatellin was detected by photochemical assay (flash-induced charge recombination of the reaction center) and the protonation/deprotonation equilibrium of the phenolic group by spectral assay monitoring the band peaks at 272 nm and 340 nm of the absorption spectra of the stigmatellin ($\Delta\varepsilon_{272}$(deprot/prot) = 10 $mM^{-1}\cdot cm^{-1}$). The dissociation constant of stigmatellin binding increased by about two orders of magnitude from 4 nM (pH 8.5) to 350 nM (pH 11.0) in chromatophores indicating the difference in binding affinities between the protonated and deprotonated forms of the stigmatellin. The observed p*K* of the phenolic proton has proved to be very sensitive to the surroundings: 9.4 (in aqueous solution), 9.4-10.3 (in different detergents) and 10.2 (in excess to RC in detergent n-octyl-β-D-glycopyranoside). This wide range of values may indicate highly different electric fields (energetic coupling with the phenolic proton of the stigmatellin) and/or solvation energy of stigmatellin in different phases of the detergent/protein/membrane system.

Acta Biol Szeged 48(1-4):25-33 (2004)

KEY WORDS

photosynthesis
chromatophore
quinones
inhibitors
electron transfer
proton binding/unbinding

Ultimately all life on earth depends on the ability of photosynthetic organisms (bacteria and higher plants) to convert solar energy into other forms of free energy directly amenable to fuel energy consuming processes (ion transport, ATP production, cell growth, etc.). The photosynthetic reaction center (RC), an integral membrane protein-pigment complex, plays a central role in this process. The RCs from purple bacteria are the best characterized of these membrane protein complexes (see Blankenship et al. 1995; Wraight 2004).

The RC performs light-induced redox chemistry: upon light excitation, the RC generates and exports oxidizing and reducing equivalents in a cyclic manner. In RCs of purple bacteria and Photosystem II of oxygenic organisms, the reducing equivalents are produced and exported in pairs, as quinol (fully reduced quinone, QH_2). The reduction of quinone (Q) by two electrons and two H^+ ions requires coordinated quinone/quinol exchange, light-induced electron transfer steps and proton transfer reactions (Fig. 1 and see Gerencsér et al. 2000). The initial step of the quinone reduction cycle is the binding of quinone from the membrane pool to the Q_B binding site of the RC. While the quinone is tightly bound (as a "prosthetic group") to the Q_A site in both oxidized (Q_A) and anionic semireduced (Q_A^-) redox states in the RC, Q_B is in weak binding equilibrium when fully oxidized (Q_B) or reduced (Q_BH_2). If, however, Q_B is reduced by light generated first electron transfer, e(1), it becomes tightly bound as semiquinone (Q_B^-). The subsequent photoactivation of the RC provides a second electron, e(2) to the quinone complex ($Q_A^-Q_B^-$). The negative charges of the anionic semiquinones induce proton binding to the protein. The first proton uptake to the quinone headgroup, H(1) creates the energetically unfavorable intermediate, $Q_A^-Q_BH$. The energetic gap between the two intermediates ($Q_A^-Q_B^-$ and $Q_A^-Q_BH$) depends on the proton equilibrium constant of the Q_B^- semiquinone (pK_1'). The range of pK_1' (≈ 5 in water and 4–6 in RCs (Graige et al. 1999; Lavergne et al. 1999)) suggests that the $Q_A^-Q_BH$ state lies 60–180 meV above $Q_A^-Q_B^-$ at pH 7, and progressively more at higher pH (60 meV per pH unit). The uphill (fast) proton transfer is followed by rate-limiting and downhill interquinone electron transfer from Q_A^- to Q_BH resulting in the $Q_A(Q_BH)^-$ intermediate that is further protonated by downhill proton transfer to produce fully reduced quinone, $Q_AQ_BH_2$. The uptake of the second proton, H(2) is kinetically indistinguishable from the first proton transfer in the wild type RC and can only be resolved in the case of mutants (e.g. GluL212→Gln, where 'L' represents the L subunit of the RC),

Accepted Apr 16, 2004
*Corresponding author. E-mail: pmaroti@sol.cc.u-szeged.hu

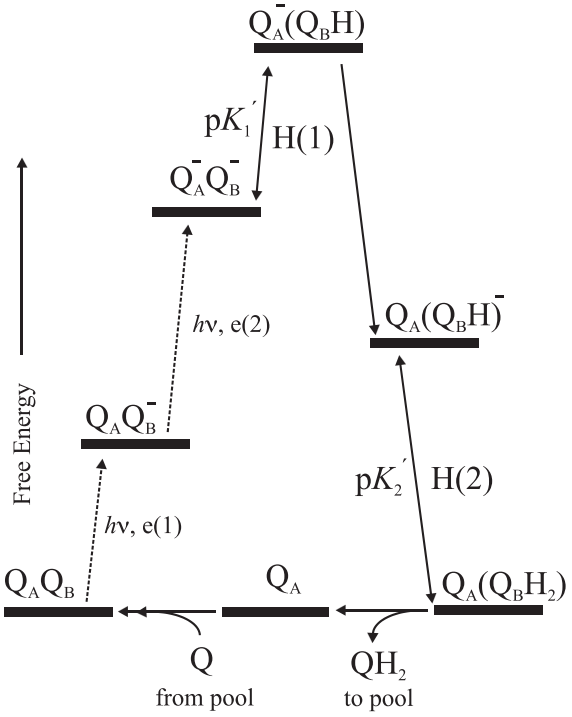

Figure 1. Relative free energy levels of the redox states of the Q_AQ_B quinone acceptor complex involved in the light-induced reduction cycle in RC of photosynthetic bacteria. Notations: *hν*: light driven reaction; e(1) and e(2): first and second electron injected to the quinone complex, respectively; H(1) and H(2): first and second H^+ ion bound to Q_B via equilibrium constants of pK_1' and pK_2' of the Q_AQ_B quinone acceptor complex, respectively.

with significantly retarded second proton uptake rates (Paddock et al. 1989; Takahashi and Wraight 1992; McPherson et al. 1994). The ubiquinol then leaves its binding site and is replaced by quinone from the membrane pool, and the turnover of the quinone complex can be started again.

The protonation and the p*K* values of the different forms of the semiquinone in the photocycle have been one of the ongoing problems of RC research. The absorption spectrum of the (first) flash-induced $Q_AQ_B^-$ state in isolated RC (with a characteristic peak at 450 nm) indicates that the semiquinone exists in fully anionic (unprotonated) redox state down to pH ≈ 3.5, a lower limit for RC protein. This means that the pK($Q_AQ_B^-$) should be smaller than 3.5. It is much more difficult to determine the p*K* value of Q_B^- after the second flash, when the primary quinone is in reduced state. The protonated species $Q_A^-Q_BH$ is present only at low levels (due to the low p*K* value) even at acidic pH and is short lived due to the very rapid reduction to $Q_AQ_BH^-$ (see the photocycle). Graige et al. (1999) were able to overcome this problem when they replaced the native ubiquinone at the Q_B site by rhodoquinone (RQ) that had a much higher solution p*K* (≈ 7.2) than the ubiquinone. The direct protonation of the semiquinone after the first flash could be observed and pK(Q_ARQ^-) ≈ 7.2 value was determined. After the second flash, they observed a regular pH-dependence of the second electron transfer rate with pK($Q_A^-RQ^-$) ≈ 8.0. The upshift is $\Delta pK(Q_A^-RQ^-/Q_ARQ^-)$ = 0.8. By comparing the behavior with RQ and ubiquinone, they suggested pK($Q_A^-Q_B^-$) ≈ 4.5-5.0 for native ubiquinone at pH 7.5. This value is very similar to the p*K* estimated for ubisemiquinone in water (pK = 4.9, Wraight 2004). It should be noted that, based on the pH-dependence of the rate of the second electron transfer, the pK($Q_A^-Q_B^-$) is not constant but is continuously modulated by interactions with changing electrostatic protein environment (different protonatable groups with different p*K* values become deprotonated upon increase of the pH).

One of the key steps of the quinone reduction photocycle is the exchange of quinone for quinol. During this process, several herbicides are able to replace the quinone by competitive binding to the Q_B site, thereby blocking the photocycle (Tischer and Strotman 1977; Wraight 1981; Stein et al. 1984; Vermaas et al. 1984; Oettmeier and Preusse 1987; Paddock et al. 1988). Over 50% of commercially available herbicides function by inhibition of higher plants at the Q_B site on the D1 polypeptide of the photosystem II RC (Percival and Baker 1991). Many herbicides are triazines (e.g. atrazine, terbutryne). The triazine binding site has been localized by X-ray crystallographic analysis of the RC-terbutryne complex at a resolution of 2.9 Å (Michel et al. 1986). High quality structural data have been collected on RC complexes with atrazine and two chiral atrazine derivatives paving the way for detailed description of the triazine type inhibitor binding (Lancaster and Michel 1996).

Other inhibitors of Q_B function more closely resemble quinones in structure. Among these compounds, the antibiotic stigmatellin is the most widely used (Fig. 2). The chromone-type stigmatellin is characterized by three unique and useful properties. a) It is a potent electron transfer inhibitor in several redox proteins of bioenergetic membranes. In addition inhibiting quinone reduction in bacterial RCs (Giangiacomo et al. 1987; Oettmeier and Preusse 1987) and in photosystem II (Oettmeier et al. 1985), stigmatellin is a very active inhibitor of quinol oxidation in the cytochrome bc_1 complex. The dissociation constants (K_S value) for stigmatellin at the Q_B site of isolated RC from *Rhodobacter sphaeroides* is reported to be ≈ 50 nM (von Jagow and Ohnishi 1985), whereas the 50% inhibition (I_{50}) value is ≈ 1.5 μM for RCs in native membranes (chromatophores; Giangiacomo et al. 1987). In chromatophores of *Rb. capsulatus*, the inhibition of the stigmatellin was found to be much greater than that of terbutryne (the K_S values are 0.37 μM and 6.0 μM, respectively) and the release time of stigmatellin from the Q_B binding site is much larger than that of terbutryne (≈ 30 s and 80 ms, respectively; Ginet and Lavergne 2001). b) The protonation state of the stigmatellin can be followed by absorption spectroscopy and the pK_a of the titrating site is estimated as 9.3 in aqueous

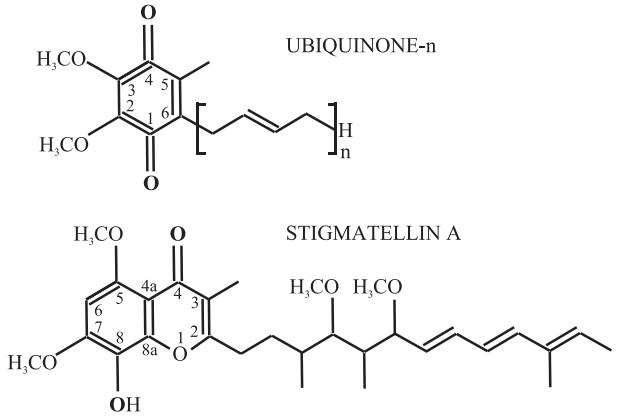

Figure 2. Chemical structures of ubiquinone and stigmatellin. Both have high binding affinity to the Q_B site of the photosynthetic RC. The native ubiquinones of *Rp. viridis* and *Rb. sphaeroides* are ubiquinone-9 and ubiquinone-10, respectively. The keto oxygens of ubiquinone can be protonated during the quinone reduction cycle and the hydroxyl group of the stigmatellin can be deprotonated in the alkaline pH region. See the structural similarity between the monoprotonated semiquinone and the stigmatellin.

solution (Graige et al. 1996). The pK_a of the phenolic proton of the stigmatellin is sensitive to the environment, and it can potentially be used as a probe of the local electrostatics. c) Comparing the chemical structures and binding positions of the quinones and the antibiotic stigmatellin, it appears that stigmatellin resembles the protonated semiquinone at lower pH (< 8) and the semiquinone anion radical at higher pH (> 10). These quinone redox states are essential intermediates in the quinone reduction photocycle (Fig. 1). However, they (especially the protonated semiquinone) are not readily accessible by direct spectroscopic and kinetics methods (Wraight 2004), and stigmatellin may provide some insight to the modes of binding and interactions of semiquinones in the photocycle of the RC. The present study addresses these three aspects of stigmatellin in bacterial RC protein both in native membrane (chromatophores) and in detergent solution.

Materials and Methods

Reagents, bacterial strains, chromatophores and RCs

The stability of the stigmatellin is limited in aqueous solution and after prolonged incubation (days) in aqueous solution, the stigmatellin looses its phenolic group: the 340 nm band gradually diminishes and disappears. To avoid this problem, fresh stigmatellin (Fluka) was always taken from a non-aqueous stock (4 mM in ethanol). To stabilize the pH of the sample solution, 2-10 mM pH buffers were used (Tris, Ches or Caps (all from Sigma) depending on the pH).

The carotenoidless R-26 strain of the photosynthetic bacterium *Rhodobacter sphaeroides* was grown under photoheterotrophic and anaerobic conditions in medium supplemented with potassium succinate. The nonphotosynthetic strain of the double mutant of *Rhodobacter sphaeroides* 2.4.1, CYCA1 (a kind gift of Prof. Donohue, Madison, Wisconsin USA) is deleted in cytochrome c_2. It was grown aerobically in darkness in Hutner medium supplemented with kanamycin corresponding to the antibiotic resistance cassette associated with the deletions.

To prepare chromatophores from CYCA1, the cells were washed, suspended in 100 mM KCl and 10 mM Tris buffer (pH 8.0) and broken by sonication. Unbroken cells were eliminated by centrifugation (17,000 g, 15 min). The supernatant was spun at 200,000g for 90 min. The chromatophore pellet was resuspended in a medium of minimum volume containing 1 mM Tris and 100 mM KCl. Samples were diluted 10-50 times for measurements.

Isolation of RC from R-26 chromatophore followed standard procedure (Maróti and Wraight 1988). The protein was solubilized by the zwitterionic detergent LDAO (N,N-dimethyldodecylamine-N-oxide, Fluka) and purified by ammonium sulfate precipitation steps followed by DEAE Sephacel (Sigma) anion exchange column chromatography. The fractions of purity (OD_{280}/OD_{802}=) 1.30 were collected. To exchange the zwitterionic detergent (LDAO) for a non-ionic one (e.g. Triton X-100), the RC preparation was dialyzed against 1 mM Tris buffer (pH 8.0) and 0.03% Triton X-100 overnight at 4°C under heavy stirring.

Optical spectroscopy

The pH-dependence of the absorption spectrum of the stigmatellin was determined (with and without RCs or chromatophores) from the steady state spectrum, measured with a dual beam absorption spectrophotometer (Unicam 4A). The relatively small absorption change of the stigmatellin ($\Delta A \approx$ 10 mOD) had to be detected in a background of large ($A \approx 1$ OD), pH-dependent and overlapping absorption of the RC (or chromatophores) in the UV and visible range where scattering could be substantial. To reduce this technical difficulty, near field (close to the photodetector) observation was applied. The reference and sample were made identical by splitting the stock solution with buffers, RC (and detergent) or chromatophores into two halves and the baseline was recorded (usually at pH 8). Then stigmatellin was added to the sample cuvette and an identical volume of ethanol to the reference cuvette. The pH values of both solutions were measured by calibrated glass electrodes immersed into the 1-1 cm cuvettes, and adjusted to the same pH value by addition of small (1-5 µl) amounts of concentrated (1 M) HCl or NaOH solutions.

Flash-induced absorption changes were detected by a single beam spectrophotometer of local design (Maróti and Wraight, 1988). The charge recombination kinetics were followed at 865 nm (isolated RC, $\Delta\varepsilon(865) = 112\ mM^{-1}\cdot cm^{-1}$) or at 603 nm (chromatophores, $\Delta\varepsilon(603) = 20\ mM^{-1}\cdot cm^{-1}$). Usu-

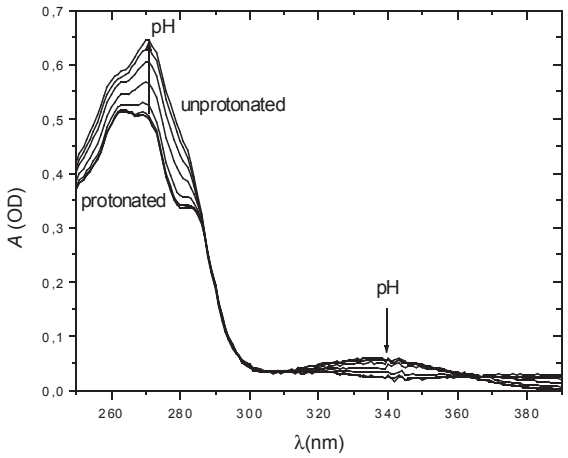

Figure 3. Absorption spectra of stigmatellin at different pH values. The arrows at two characteristic peaks (272 nm and 340 nm) indicate the direction of change of the bands upon pH increase from 6.8 to 12.05. The spectra of protonated and deprotonated forms of stigmatellin are shown at pH values much below and above the p*K* (= 10.3), respectively. Conditions: 11 μM stigmatellin, 0.03% TX-100 and 1-1 mM Tris, Ches and Caps.

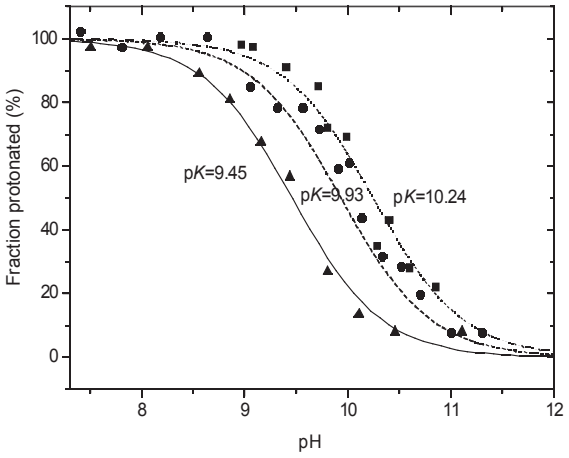

Figure 4. pH-titration of the stigmatellin based on the difference of the steady-state absorption spectra of the protonated/unprotonated forms in different environments: in water (▲), in detergent n-octyl-β-D-glycopyranoside (●) and in detergent n-octyl-β-D-glycopyranoside + RC (■). The (solid, dashes and dotted) lines indicate fits of the measured data (in water, detergent and RC, respectively) by Henderson-Hasselbalch function of characteristic of the protonation equilibrium of a single and independent protonatable group. Conditions: ▲ (5 μM stigmatellin, 2-2 mM Tris and Ches, λ = 272 nm), ● (10 μM stigmatellin, 20 mM n-octyl-β-D-glycopyranoside, 2-2 mM Tris and Caps, λ = 272 nm), ■ (10 and 13 μM stigmatellin in the reference and in the sample, respectively, 3.46 μM RC, 20 mM n-octyl-β-D-glycopyranoside and 2-2 mM Tris and Caps. The fraction of protonated stigmatellin was determined form the shape of the absorption spectrum.) The reference was identical to that of the sample except of (access) stigmatellin in the sample (the same volume of ethanol was added to the reference). The zero line of the spectrum was adjusted before addition of access stigmatellin to the sample at pH 8.4.

ally, they showed two (fast and slow) components revealed by biexponential decomposition of the trace via Levenberg-Marquardt non-linear fitting:

$$A=A_{fast}\cdot\exp(-k_{fast}t)+A_{slow}\cdot\exp(-k_{slow}t) \quad (1)$$

Here A and k are the amplitudes and rate constants of the components, respectively. Using the firmly bound quinone (stigmatellin) model (see Appendix), the fast component is characteristic of the charge recombination from the reduced primary quinone (blocked Q_B site, $P^+Q_A^- \rightarrow PQ_A$), while the slow phase describes charge recombination from an acceptor quinone complex where the electron is shared between the two quinones: $P^+(Q_AQ_B)^- \rightarrow P(Q_AQ_B)$ (Wraight and Stein 1983; Kleinfeld et al. 1984).

Table 1. p*K* values of phenolic proton of stigmatellin dissolved in different detergents.

Detergents		p*K*
Water		9.4
LDAO (zwitterionic)		
	0.020 %	10.3
Triton X-100 (non-ionic)		
	0.005 %	9.65
	0.010 %	10.15
	0.020 %	10.3
	0.030 %	10.3
n-octyl-β-D-glycopyranoside (non-ionic)	1 mM	9.4
	5 mM	9.7
	10 mM	9.8
	20 mM (cmc)	10.0

Results

Spectral assay

Our experiments demonstrate that the steady-state absorption spectrum of the stigmatellin is pH-dependent, and indicates the distribution between its ionized (deprotonated) and protonated forms (Fig. 3). The near-UV absorption spectrum of stigmatellin shows characteristic bands at 272 nm (strong and narrow) and at 340 nm (much weaker and wider). Whereas the 272 nm band is one component of a complex UV band, the 340 nm band is a relatively isolated, single peak. Both bands are very sensitive to pH in the interval close to the p*K* value of the hydroxyl group of the molecule (Fig. 2). The absorption spectra recorded at different pH values show an isosbestic point around 300 nm, clearly indicating the interconversion of two absorbing species with maxima at 272 and 340 nm. Upon deprotonation (pH increase), the 340 nm band disappears completely, and the 272 nm band increases. By comparison of the absorption spectra of the fully protonated and unprotonated forms of the stigmatellin, the absorption peak at 272 nm can be calibrated: $\varepsilon_{272\ nm}$ (unprotonated) = 54 $mM^{-1}\cdot cm^{-1}$ and $\varepsilon_{272\ nm}$(protonated) = 44 $mM^{-1}\cdot cm^{-1}$, thus $\Delta\varepsilon_{272\ nm}$ (unprotonated – protonated) = 10 $mM^{-1}\cdot cm^{-1}$. These

values can be used for estimation of the ratio of the ionized and protonated forms.

The p*K* of the phenolic proton of stigmatellin is very sensitive to the environment. Figure 4 shows three pH-titrations of stigmatellin under different conditions. The pH-dependences of the fraction of protonated stigmatellin can be well approximated by a set of Henderson-Hasselbalch curves corresponding to a single protonatable group with a single p*K* value that changes according to the environment. We observed p*K* values of 9.4, 9.9 and 10.2 for the phenolic proton when stigmatellin is in aqueous solution, solubilized in detergent n-octyl-β-D-glycopyranoside or attached (is large access) to RC, respectively. Several additional p*K* values, measured under various conditions, are collected in Table 1. The p*K* values range over about 1 pH unit, indicating significant variation of interaction of the phenolic proton with the environment.

Photochemical assay

The binding of stigmatellin to the Q_B site can be probed by monitoring the absorption change of the flash-induced charge recombination. The appearance of the fast phase in the kinetics is indicative of stigmatellin binding (Fig. 5). Two criteria must be met for simple application of this, *i.e.*, without requiring major corrections: 1) the quinone occupancy at the Q_B site should be complete in the absence of stigmatellin at all pH values (full reconstitution of the Q_B activity), and 2) the lifetimes of the fast and slow components should be distinguishable at all (especially at very high) pH values. In the case of RC solubilized in detergent, the lifetimes of the two components at high pH values are rather close, but good signal-to-noise is obtained at high RC concentration and reliable decomposition of the kinetics can be achieved. The opposite case applies to chromatophores: the signal size is small compared to that of RC in detergent, but the slow component is much slower than the fast component (and the quinone occupancy remains close to 100%) even at pH 11. This is due to the larger free energy gap between the two quinones of the RC in chromatophores than in detergents.

We observed that the inhibitory effect of stigmatellin is pH-dependent, becoming less effective at high pH. The effect is more pronounced for RC in chromatophores than in detergent solution. Figure 5 shows systematic stigmatellin-titrations at low and high (fixed) pH values where the stigmatellin is largely protonated (pH 8.5) and deprotonated (pH ≥ 10.5). The data clearly show that the binding affinity of the stigmatellin to the RC decreases with increasing pH – by two orders of magnitude in chromatophores, but only a factor of 4 in micellar solution.

Discussions

The direct and separate measurements of binding and protonation state of stigmatellin provide the basis for determining the role of the phenolic group in the binding affinity to the Q_B site. Based on results obtained in this work and available in the literature, we will concentrate our discussion on structural and functional aspects of stigmatellin binding and on further possible benefits regarding the physical-chemical properties of protonated semiquinone in the RC.

Binding of stigmatellin

The titrations of Figure 5 show stigmatellin to be a very effective competitor of quinone at the Q_B site of the RC both in detergent and in native membranes (chromatophores). The effective quinone content was different in the two sets of experiments. In chromatophores, the ratio of the quinone and RC concentrations in the membrane is about 30, and the

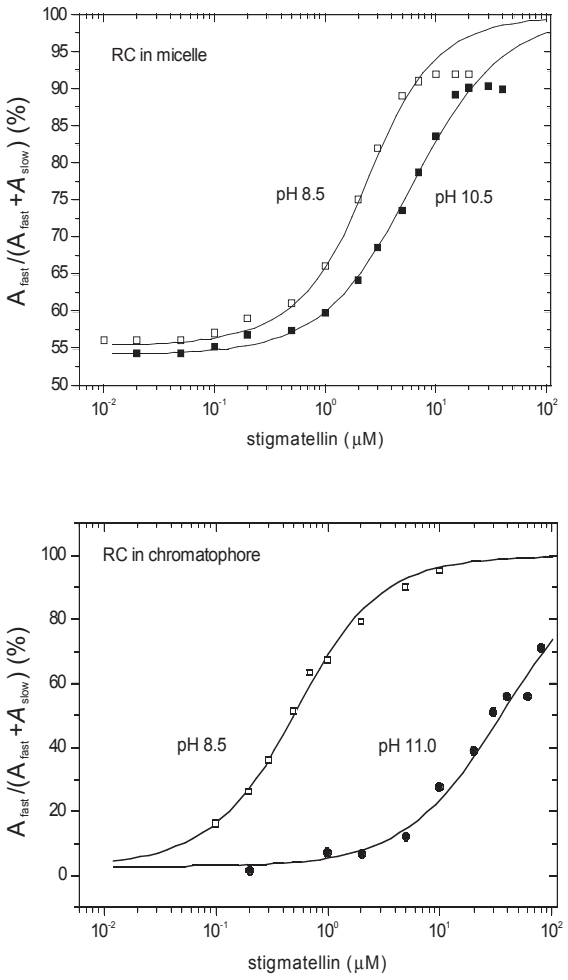

Figure 5. Concentration-dependence of the inhibitory effect of stigmatellin on photochemistry of RC in detergent Triton X-100 (top) and embedded in chromatophores of cytochrome-less mutant of *Rb. sphaeroides* (bottom). The inhibition of stigmatellin is characterized by the relative amplitude of the fast phase of the charge recombination kinetics detected at 865 nm (top) and 603 nm (bottom) after a single saturating flash excitation. Conditions: 0.03% Triton X-100, 2.21 μM RC and 5 mM Tris at pH 8.5 and 0.03% Triton X-100, 2.0 μM RC and 5 mM Caps at pH 10.5 (top), 280 nM RC, 100 mM NaCl and 10 mM Tris (bottom).

Q_B occupancy is large (only slow phase recombination can be detected even at very high pH; Fig. 5 bottom). In detergent, the quinone level was low (only endogenous Q was present, *i.e.*, no quinone was externally added) and only about half of the RC had quinone bound at the Q_B site. Somewhat surprisingly, the fraction of slow phase of the charge recombination remained unchanged upon pH increase (Fig. 5 top), even though both the quinone affinity and the interquinone one-electron equilibrium constant are strongly pH-dependent in this pH range. However, this is consistent with the low detergent concentration, in which all the quinone is present in RC-detergent mixed micelles, whether bound to the Q_B or not. Following light activation, the interquinone electron transfer equilibrium can pull unbound quinone rapidly to the Q_B site of the RC (see for details Stein et al. 1984; Shinkarev and Wraight 1997). In the presence of stigmatellin, quinone is displaced from the Q_B site, but stigmatellin unbinds very slowly so that, even after light activation, the binding pattern established in the dark (before the flash) is preserved. Thus, the titration of stigmatellin assayed by the slow recombination kinetics reflects the quinone/stigmatellin binding equilibrium in the dark-adapted state. This interpretation is supported by the slow unbinding rate of the stigmatellin (k_{off} = 0.033 s^{-1}) relative to that of the $P^+Q_A^-$–› PQ_A charge recombination (k_{fast} = 16.4 s^{-1}) observed in *Rb. capsulatus* (Ginet and Lavergne 2001).

Based on this model of a competitive, pre-flash binding equilibrium (see the Appendix), the dissociation constants of stigmatellin can be estimated. In micellar solution, using K_Q = 1.7 μM (in 0.1 % LDAO) for the dissociation constant of ubiquinone-10 (McComb et al. 1990) and [Q] = 2.4 μM, we obtain K_S = 0.4 μM at pH 8.5 and K_S = 1.8 μM at pH 10.5 for the dissociation constant of the stigmatellin. The value of K_S = 400 nM at pH 8.5 is significantly larger than that obtained earlier (50 nM) by von Jagow and Ohnishi (1985). The reason is unclear. In chromatophores, the conditions are less defined. Assuming linear partition in the membrane, thus taking bulk concentrations for the RC (300 nM) and for the size of the quinone pool (9 μM), we get K_S = 4 nM at pH 8.5 and K_S = 350 nM at pH 11.0 if K_Q = 100 nM. (Actually, K_S/K_Q ratio can be determined from the best fit. The very low amplitude of the fast phase of the charge recombination gives only an upper limit for the quinone dissociation constant: K_Q < 200 nM.)

The protonated form of stigmatellin had much higher binding affinity to the RC than the unprotonated form. As both forms are present in the pH region around the p*K* of the phenolic group, the binding pattern of the Q_B site becomes more complex: in addition to the quinone (naturally present in chromatophore), the protonated and deprotonated components of the stigmatellin compete for the same binding site. The evaluation of the model and the discussion of the consequences are challenging tasks but are beyond the capacity of this work.

The observed difference in binding affinity of the unprotonated and protonated states of the stigmatellin may be partly due to changes in the H-bond network that stabilizes the bound stigmatellin to the RC (see later) and partly to the electrostatics. The RC becomes increasingly negatively charged at higher pH, which may provide a global repulsion to the unprotonated (anionic) stigmatellin. Similarly, electrostatics may play a role in the dramatically decreased binding affinity of stigmatellin at high pH in chromatophores relative to that in detergent – the negative surface charge of the membrane may greatly diminish the effective partition coefficient for the unprotonated stigmatellin. Based on our experiments, we cannot argue that the anionic stigmatellin is less likely to partition linearly than the protonated species, just mean that the anionic partition will be smaller than the neutral form. Further investigations are needed to make sharper distinctions.

Stigmatellin bound to the Q_B pocket of the RC significantly modifies not only the function of the RC by inhibiting the electron transfer, but also perturbs interactions between the donor and acceptor sides, within the protein. In chromatophores of *Rb. capsulatus*, it has been shown that stigmatellin in the Q_B site may shift the midpoint potential ($E_{m,P}$) of the bacteriochlorophyll dimer (P/P^+) (Ginet and Lavergne 2000). The shift is significant when the primary quinone is reduced (Q_A^-): $E_{m,P}(Q_A^-\ldots)$ = 507 mV and $E_{m,P}(Q_A^-$ stig) = 449 mV, thus the shift is $\Delta E_{m,P}(Q_A^-$ stig) = 58 mV. In case of terbutryne, the shift is insignificant: $\Delta E_{m,P}(Q_A^-$ terb) = 4 mV. Thus, stigmatellin stabilizes the oxidized state of the dimer if Q_A is reduced. The interactions between P/P^+ and Q_A/Q_A^- are markedly modified by the condition of the Q_B binding pocket (empty or occupied by ubiquinone, terbutryne or stigmatellin).

Structural view of stigmatellin binding to the RC

Lancaster and Michel (1997) determined the crystal structures of RCs from *Rhodopseudomonas viridis* with ubiquinone-2 (refined at 2.45 Å resolution, PDB entry code 2PRC) and stigmatellin (refined at 2.4 Å resolution, PDB entry code 4PRC) at the Q_B binding site (Fig. 6). The geometry and the stabilizing interactions of the quinone and stigmatellin binding are similar. The quinone ring and the chromone ring of the stigmatellin are in the same plane. The stigmatellin is bound to the Q_B site with the titratable hydroxyl group at essentially the same position as a keto oxygen of the ubiquinone, the same keto oxygen that is believed to become protonated during the second electron reduction (the first protonation event) of Q_B. It appeared that the p*K* of stigmatellin was above 11 in native RC but decreased to 9.5 in L213Asp → Asn mutant RC that is very close to the value observed for stigmatellin in solution (Graige et al. 1996). Although this is a promising result to use stigmatellin as electrostatic probe of the Q_B binding site,

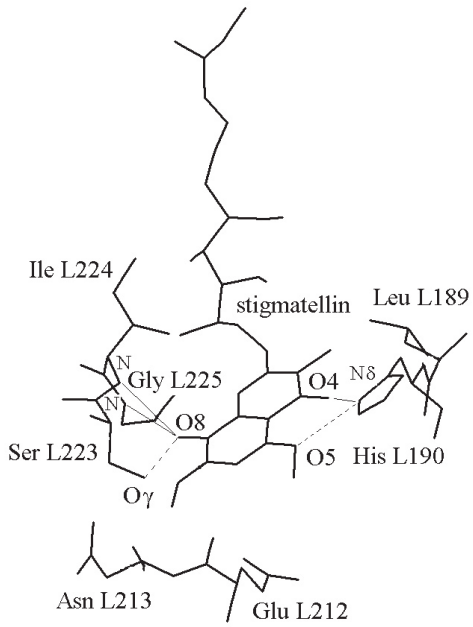

Figure 6. Stigmatellin in Q_B binding site of RC from *Rhodopseudomonas viridis* (the coordinates were taken from Protein Data Bank with accession code 4PRC). Thin solid lines: H-bond interactions present also if the binding domain is occupied by ubiquinone (His L190 Nδ – stig O4, Ile L224 N – stig O8 and Gly L225 N – stig O8) and dashed lines: extra hydrogen bonds for further stabilization of stigmatellin binding (His L190 Nδ – stig O5 and stig O8 – Ser L223 Oγ).

further investigations are needed (see below).

All of the interactions implicated in the binding of the ubiquinone headgroup are also implicated in the binding of the stigmatellin headgroup: the hydrogen bonds for quinone binding (His L190 Nδ – O4, Ile L224 N – O1 and Gly L225 N – O1) are also associated with stigmatellin binding (His L190 Nδ – O4, Ile L224 N – O8 and Gly L225 N – O8). However, two additional hydrogen bonds stabilize the binding of stigmatellin over that of ubiquinone. First, the stigmatellin proximal methoxy oxygen atom (O5) can act as a second acceptor of a hydrogen bond from the His L190 Nδ atom. Second, the Ser L223 Oγ atom accepts a hydrogen bond from the stigmatellin hydroxyl group (O8). These two additional hydrogen bonding interactions may explain the higher affinity of stigmatellin to the Q_B site as compared to quinone in RCs from *Rb. sphaeroides* (Giangiacomo et al. 1987). The hydrogen bond interaction with Ser L223 Oγ seems to be crucial in stigmatellin binding, as mutation of Ser L223 to Ala made the RC of *Rb. sphaeroides* resistant to stigmatellin (Paddock et al. 1995). The distances between H-bonding donors and acceptors can be derived from the *Rp. viridis* RC-stigmatellin structure data (PDB code 4PRC) and are listed in Table 2. The distances are short enough (average of 3.0 Å) to assure relatively strong H-bonds. The Oγ atom of Ser L223 is closest to the hydroxyl group (O8) of the stigmatellin (2.8 Å), and most likely makes the strongest H-bond.

If the ambient pH exceeds pK, the level of anionic stigmatellin becomes significant. Deprotonation of the hydroxyl group of the stigmatellin weakens the binding affinity via loss of H-bond donation from the stigmatellin to Ser L223 Oγ (stigmatellin is the proton donor) and by straightforward coulombic forces. On the other hand, deprotonation of the stigmatellin strengthens H-bond donation from the Ile L224 N and Gly L225 peptide NH groups (they are hydrogen-binding donors). These effects together will cause pH-dependent change of the binding affinity of stigmatellin to the Q_B binding site as was observed in our experiments. We might expect that the relatively small distinction between the affinity for protonated and unprotonated stigmatellin seen in isolated RCs more closely reflects the purely structural influences of the Q_B site, whereas the much greater distinction seen in chromatophores includes more extensive electrostatic influences in the membrane phase.

Stigmatellin as possible electrostatic probe

The measured pK values of the OH group of the stigmatellin showed large variation in different environments indicating sensitive changes of the interactions (Fig. 4 and Table 1). The interaction energy between the stigmatellin and the environment can include solvation energy of the stigmatellin in different (aqueous, detergent, membrane) phases, loose association (nonspecific binding, Kálmán et al. 1997) with the RC protein or electrostatic energy. If the last term dominates the interaction (or the other terms can be separated) then the stigmatellin may work like a molecular probe of the environment. The observed pK shift of the phenolic proton, ΔpK, is a direct indicator of the change in the prevailing electrostatic potential, $\Delta\psi$:

$$\Delta pK = -\frac{\Delta\psi}{60\ \text{mV}} \qquad (2)$$

Here, the proportionality factor 60 mV is calculated from the Boltzmann expression for the thermal energy ($2.303k_BT$) at room temperature. One unit of pK shift corresponds to –60 mV change in electrostatic potential. $\Delta pK \approx 0.3$ pH unit

Table 2. Distances between hydrogen-bonding donors (D) and acceptors (A) in the Q_B site for *Rp. viridis* RC-stigmatellin crystals (Protein Data Bank with accession code 4PRC).

D	A	D-A (Å)
His L190 Nδ	Stig O4	2.7
His L190 Nδ	Stig O5	3.1
Ile L224 N	Stig O8	3.0
Gly L225 N	Stig O8	3.1
Stig O8	Ser L223 Oγ	2.8

upshift is observed in RC relative to that in detergent (n-octyl-β-D-glycopyranoside) that might be a consequence of negative surface potential of the protein ($\Delta\psi \approx -20$ mV).

It would be more interesting and important to probe inside the binding pocket. Preliminary experiments indicate that no major changes can be observed between p*K* values of stigmatellin inside (added in stoichiometric quantity to the RC) and outside (added in large access to the RC). However, we can predict significant changes if the electrostatics of the binding pocket is artificially modified by site-directed mutagenesis of key amino acids. Graige et al. (1996) removed a negative charge from the vicinity of the bound stigmatellin by mutation of Asp for Asn at position L213 (AspL213 → Asn) and the p*K* downshifted from an unidentified high value (p$K >> 10.6$) to about 10, a value closer to the "solutional" p*K*. Assuming that this p*K* downshift comes from a single strong Coulombic interaction between the negative charges on the carboxylate of AspL213 and carbonyl oxygen of the stigmatellin, the effective potential at O8 can be calculated:

$$\Delta\psi = \frac{1}{4\pi\varepsilon_0} \cdot \frac{e}{\varepsilon_r \cdot r} \qquad (3)$$

where e is the elementary charge ($e = 1.6 \cdot 10^{-19}$ C), ε_0 (= $8.854 \cdot 10^{-12}$ As/Vm) and ε_r are the absolute and relative dielectric constants, respectively, and r is the (average) distance between O8 of the stigmatellin and the carboxylic oxygens of AspL213. Using $\Delta pK \geq -1.5$, *i.e.* based on Eq. (2) $\Delta\psi \geq +90$ mV and $r = 7$ Å (obtained from the 4PRC crystal structure), we obtain rather small value for the effective dielectric constant: $\varepsilon_r < 20$. This indicates that the interaction is only moderately screened by polarizable molecules. The stigmatellin (and also the native ubiquinone) is bound to a highly hydrophobic region of the Q_B binding pocket and the X-ray structures reveal only very few water molecules in the immediate vicinity.

Appendix

Scheme of binding equilibrium between quinone (Q) and stigmatellin (S) to the Q_B site of the RC in the oxidized state of the primary quinone Q_A (in the dark or under pre-flash conditions):

$$Q_AS \xleftarrow{K_S} Q_A \xleftarrow{K_Q} Q_AQ_B$$

Here K_S and K_Q are the dissociation constants of the stigmatellin and quinone, respectively. The RC, the quinone and the stigmatellin can be found either in free or in bound forms, thus their total amounts (concentrations, denoted by [..]) can be expressed as

$$[RC_{total}]=[Q_AS]+[Q_A]+[Q_AQ_B] \qquad (A1)$$
$$[Q_{total}]=[Q_{free}]+[Q_AQ_B] \qquad (A2)$$
$$[S_{total}]=[S_{free}]+[Q_AS] \qquad (A3)$$

Under steady-state conditions

$$[Q_A]\cdot[S_{free}] = K_S\cdot[Q_AS] \qquad (A4)$$
$$[Q_A]\cdot[Q_{free}] = K_Q\cdot[Q_AQ_B] \qquad (A5)$$

There are 5 unknown quantities ($[Q_A]$, $[Q_{free}]$, $[S_{free}]$, $[Q_AS]$ and $[Q_AQ_B]$) and 5 equations which are solved numerically using MatCad 4.0 (Fig. 5)

Acknowledgments

This work was supported by OTKA (T-42680), TéT (I-46/99 and F-34/02), NSF (MCB 03-44449) and MTA-NSF (042/2000).

References

Blankenship RE, Madigan MT, Bauer CE (1995) *Anoxygenic Photosynthetic Bacteria.* Kluwer Academic Publishers, Dordrecht, The Netherlands.

Gerencsér L, Jánosi T, Laczkó G, Maróti P (2000) Kinetic limitations in turnover of photosynthetic bacterial reaction center protein. Acta Biol Szeged 44:45-52.

Giangiacomo KM, Robertson DE, Gunner MR, Dutton PL (1987) Stigmatellin and other Electron Transfer Inhibitors as Probes for the Q_B Binding Site in the Reaction Center of Photosynthetic Bacteria. In Biggins J ed., Progress in Photosynthesis Research. Martinus Nijhoff Publishers, Dordrecht, The Netherlands, pp. 409-412.

Ginet N, Lavergne J (2000) Interactions between the Donor and Acceptor Sides in Bacterial Reaction Centers. Biochemistry 39:16252-16262.

Ginet N, Lavergne J (2001) Equilibrium and Kinetic Parameters for the Binding of Inhibitors to the Q_B Pocket in Bacterial Chromatophores: Dependence on the State of Q_A. Biochemistry 40:1812-1823.

Graige MS, Paddock ML, Feher G, Okamura MY (1996) Using Stigmatellin to Probe the Electrostatic Environment of the Q_B Site in Bacterial RCs. Biophys J (Abstracts) 70: A11 (Abstr. # Su-AM-G7, 40th Annual Meeting of the Biophysical Society, in Baltimore, MD, February 17-21, 1996).

Graige MS, Paddock ML, Feher G, Okamura MY (1999) Observation of the Protonated Semiquinone Intermediate in Isolated Reaction Centers from *Rhodobacter sphaeroides:* Implications for the Mechanism of Electron and Proton Transfer in Proteins. Biochemistry 38:11465-11473.

Kálmán L, Gajda T, Sebban P, Maróti P (1997) pH-metric study of reaction centers from photosynthetic bacteria in micellar solutions: protonatable groups equilibrate with the aqueous bulk phase. Biochemistry 36:4489-4496.

Kleinfeld D, Okamura MY, Feher G (1984) Electron transfer in reaction centers of *Rhodopseudomonas sphaeroides* I. Determination of the charge recombination pathway of $D^+Q_AQ_B^-$ and free energy and kinetic relations between $Q_A^-Q_B$ and $Q_AQ_B^-$. Biochim Biophys Acta 766:126-140.

Lancaster CR, Michel H (1996) New insights into the X-ray structure of the reaction center from *Rhodopseudomonas viridis*. In: Reaction Centers of Photosynthetic Bacteria. Structure and Dynamics. Michel-Beyerle ME ed. Springer Verlag, Berlin, pp. 23-35.

Lancaster CR, Michel H (1997) The coupling of light-induced electron transfer and proton uptake as derived from crystal structures of reaction centres from *Rhodopseudomonas viridis* modified at the binding site of the secondary quinone, Q_B. Structure 5:1339-1359.

Lavergne J, Matthews C, Ginet N (1999) Electron and Proton Transfer on the Acceptor Side of the Reaction Center in Chromatophores of *Rhodobacter capsulatus:* Evidence for Direct Protonation of the Semiquinone State of Q_B. Biochemistry 38:4542-4552.

Maróti P, Wraight CA (1988) Flash-induced H^+ binding by bacterial photosynthetic reaction centers: Comparison of spectrophotometric and conductimetric methods. Biochim Biophys Acta 934:314-328.

McComb JC, Stein RR, Wraight CA (1990) Investigations on the influence of headgroup substitution and isoprene side-chain length in the function of primary and secondary quinines of bacterial reaction centers. Biochim Biophys Acta 1015:156-171.

McPherson PH, Schönfeld M, Paddock ML, Okamura MY, Feher G (1994) Protonation and free energy changes associated with formation of Q_BH_2 in native and Glu-L212→Gln mutant reaction centers from *Rhodobacter sphaeroides.* Biochemistry 33:1181-1193.

Michel H, Epp O, Deisenhofer J (1986) Pigment protein interactions in the photosynthetic reaction centre from *Rhodopseudomonas viridis*. EMBO J 5:2445-2451.

Oettmeier W, Godde D, Kunze B, Höfle G (1985) Stigmatellin. A dual type inhibitor of photosynthetic electron transport. Biochim Biophys Acta 807:216-219.

Oettmeier W, Preusse S (1987) Herbicide and quinone binding to chromatophores and reaction centers from *Rhodobacter sphaeroides*. Z Naturforsch 42c:690-692.

Paddock ML, Rongey SH, Abresch EC, Feher G, Okamura MY (1988) Reaction centers from three herbicide-resistant mutants of *Rhodobacter sphaeroides* 2.4.1: sequence analysis and preliminary characterization. Photosynth Res 17:75-96.

Paddock ML, Rongey SH, Feher G, Okamura MY (1989) Pathway of proton transfer in bacterial reaction centers: Replacement of glutamic acid 212 in the L subunit by glutamine inhibits quinone (secondary acceptor) turnover. Proc Natl Acad Sci USA 86:6602-6606.

Paddock ML, Feher G, Okamura MY (1995) Pathway of proton transfer in bacterial reaction centers: further investigations on the role of Ser L223 studied by site-directed mutagenesis. Biochemistry 34:15742-15750.

Percival MP, Baker NR (1991) Herbicides and photosynthesis. In: Baker NR, Percival MP eds. Herbicides pp. 1-26. Elsevier Science Publishers, Amsterdam, The Netherlands.

Shinkarev VP, Wraight CA (1997) The interaction of quinone and detergent with reaction centers of purple bacteria. 1. Slow quinone exchange between reaction center micelles and pure detergent micelles. Biophys J 72:2304-2319.

Stein RR, Castellvi AL, Bogacz JP, Wraight CA (1984) Herbicide-Quinone Competition in the Acceptor Complex of Photosynthetic Reaction Centers From *Rhodopseudomonas sphaeroides*: A Bacterial Model for PS-II-Herbicide Activity in Plants. J Cell Biochem 24:243-259.

Takahashi E, Wraight CA (1992) Proton and Electron Transfer in the Acceptor Quinone Complex of *Rhodobacter sphaeroides* Reaction Centers: Characterization of Site-Directed Mutants of the Two Ionizable Residues, Glu^{L212} and Asp^{L213}, in the Q_B Binding Site. Biochemistry 31(3):855-866.

Tischer W, Srotman H (1977) Relationship between inhibitor binding by chloroplasts and inhibition of photosynthetic electron transport. Biochim Biophys Acta 460:113-125.

Von Jagow G, Ohnishi T (1985) The chromone inhibitor stigmatellin-binding to the ubiquinol oxidation center at the C-side of the mitochondrial membrane. FEBS Lett 185:311-315.

Vermaas WFJ, Renger G, Arntzen CJ (1984) Herbicide/quinone binding interactions in photosystem II. Z Naturforsch 39c:368-373.

Wraight CA (1981) Oxidation-Reduction Physical Chemistry of the Acceptor Quinone Complex in Bacterial Photosynthetic Reaction Centers: Evidence for a New Model of Herbicide Activity. Israel J Chem 21:348-354.

Wraight CA, Stein RR (1983) Bacterial reaction centers as a model for photosystem II: turnover of the secondary acceptor quinone. In: Inoue Y, Crofts AR, Govindjee, Murata N, Renger G, Satoh K eds. The Oxygen Evolving System of Photosynthesis pp. 383-397. Academic Press, New York.

Wraight CA (2004) Proton and Electron Transfer in the Acceptor Quinone Complex of Bacterial Reaction Centers. Front Biosci 9:309-337.